

A polarographic, oxygen-selective, vibrating-microelectrode system for the spatial and temporal characterisation of transmembrane oxygen fluxes in plants

Stefano Mancuso¹, Giorgio Papeschi², Anna Maria Marras²

¹Dipartimento di Ortoflorofruitticoltura, Università di Firenze, via Gaetano Donizetti 6, 50144 Florence, Italy

²Dipartimento di Scienze Farmaceutiche, Università di Firenze, via Gino Capponi 9, 50122 Florence, Italy

Received: 12 November 1999 / Accepted: 1 February 2000

Abstract. A simple procedure is described for the fabrication of micrometer to nanometer-scale platinum electrodes to be used in a vibrating oxygen-selective system. The electrode was prepared by etching a fine platinum wire and insulating it with an electrophoretic paint. The dimensions allowed this electrode to be used with the “vibrating probe technique” in exploratory studies aimed at mapping and measuring the patterns of net influxes as well as effluxes of oxygen in *Olea europaea* L. leaves and roots with spatial and temporal resolutions of a few microns and a few seconds, respectively. The magnitude and spatial localisation of O₂ influxes in roots was characterised by two distinct peaks. The first, in the division zone, averaged $38 \pm 5 \text{ nmol m}^{-2} \text{ s}^{-1}$; the second, in the elongation region, averaged $68 \pm 6 \text{ nmol m}^{-2} \text{ s}^{-1}$. Long-term records of oxygen influx in the elongation region of the root showed an oscillatory regime characterised by a fast oscillation with periods of about 8–9 min. In leaves, the system allowed the measurement of real-time changes in O₂ evolution following changes in light. Furthermore, it was possible to obtain “topographical” images of the photosynthetically generated oxygen diffusing through different stomata from a region of the leaf of $120 \mu\text{m} \times 120 \mu\text{m}$. The combination of topographic and electrochemical information at the micrometer scale makes the system an efficient tool for studying biological phenomena involving oxygen diffusion.

Key words: *Olea europaea* (O₂ flux) – Oscillation (O₂ flux) – Oxygen flux – Oxygen-selective microelectrode – Photosynthesis – Root (O₂ flux)

Introduction

The experimental measurement of cellular O₂ levels in plants is fundamental when discriminating normal physiological function from abnormal or stressed states. Several commercially available O₂ macro-sensors can be used to obtain estimates and to characterise oxygen fluxes in higher-plant cells. However, these all integrate fluxes over the entire surface of the tissue, and provide a flux representing an average value over the period of measurement. Consequently, these techniques have a spatial and temporal resolution not adequate for studying the oxygen metabolism at the single-cell level. Microelectrodes, also, have been used for many years for direct measurements of tissue oxygenation in animal and plant studies (Armstrong 1994; Ober and Sharp 1996). Nevertheless, invasive measurements are unsatisfactory for the experimental errors generated both by the damage and the stress response of the cells probed.

In recent years, the manufacture and use of electrodes with characteristic dimensions in the micrometer to nanometer range has become more widespread (Penner et al. 1990). There are a variety of techniques which now allow the production of very tiny electrodes. Many of these procedures arise from the development of tips used for scanning tunnelling microscopy or scanning electrochemical microscopy in solution (Bard et al. 1989; Frateur et al. 1999) and are interesting to us because the tips are typically constructed from platinum or platinum-iridium microwires, the same material used for the manufacture of an oxygen cathode. The wires are usually electrochemically etched to a sharp point, and then coated with an insulating material, except at the very apex of the tip, thus providing a very small exposed electrode area.

Concurrent with the increasing use of microelectrodes in many areas of plant physiology, the development of the vibrating self-referencing electrode technique (Jaffe and Nuccitelli 1974), later adapted for use with various ion-selective electrodes, has facilitated precise non-invasive measurements of ion fluxes in roots (e.g. Kochian et al. 1992; Shabala et al. 1997; Piñeros et al. 1998;

Shabala and Newman 1998), leaves (Shabala and Newman 1999) and protoplasts (Shabala et al. 1998). The inherent advantage of this approach is basic: it enables one to measure ion fluxes directly, and it does this simply, quickly, and in a continuous and non-invasive manner.

Recently, Land et al. (1999) succeeded in measuring oxygen fluxes in an isolated neuron and in the filamentous alga *Spirogyra greveilina*, taking advantage of the vibrating-electrode technology combined with the use of a membrane-tipped, polarographic oxygen microelectrode of the type developed by Whalen et al. (1967).

In the present work we describe a simple, inexpensive and highly successful procedure for the construction of platinum electrodes with dimensions in the range of micrometers to be used as O₂-selective electrodes. The use of these microelectrodes coupled with the vibrating-probe technique gives us the means to monitor oxygen dynamics associated with single cells located at the surface of plant tissues, allowing the study of spatial and temporal differences and/or relationships which can not be detected by standard O₂-measurement systems.

Materials and methods

Plant material. Cuttings from 1-year-old shoots, 12–15 cm long and with six leaves, were taken from 7-year-old stock plants of *Olea europaea* L. cv. Leccino.

In order to favour rooting, the lower portion of each cutting was immersed to a depth of 5 mm, in an aqueous KIBA (potassium salt of 3-indolebutyric acid) solution at 3600 µg ml⁻¹ for 5 s. The cuttings were then placed in an inert medium of perlite and kept in a greenhouse under conditions of high relative humidity (mist propagation), daylight for 12 h and average diurnal and nocturnal temperatures of 22 °C and 15 °C, respectively. Rooting took 8 weeks. At the end of the rooting period, plants with roots of uniform length (2–3 cm), thickness (1–2 mm), and colour (white) were chosen. After removing the perlite residue, the root systems of entire plants were immersed, under weak illumination, in an aerated nutrient solution composed of: 1 mM KCl, 0.905 mM NaH₂PO₄, 0.048 mM Na₂HPO₄, 1 mM Ca(NO₃)₂, 0.25 mM MgSO₄. The solution temperature was maintained at 25 ± 1 °C for the immersion period. The plants were then utilised for the experiments.

Electrode fabrication. The procedure for the fabrication of the platinum microcathode is outlined in Fig. 1. A platinum wire 10 mm long and 0.2 mm in diameter was soldered to a silver connecting wire of the same diameter. This assembly was then mounted in a glass capillary (2 mm o.d., 1.12 mm i.d.; World Precision Instruments, Sarasota, Fla., USA) such that approximately 3 mm of the platinum wire protruded from the capillary tip. The microwire was secured in position by melting the glass tip of the capillary around the wire. The resulting ensemble is illustrated in Fig. 1A.

Etching of the protruding wire to form a sharp tip was accomplished galvanically using the following procedure. The end 2 mm of the wire was submerged in the electrochemical etching mixture composed of KNO₃ + 5% KHCO₃ (1:19, W/W) melted at 600 °C. A current flow of 1.3 A was applied between the microwire and a platinum laminar anode of about 1 cm² (Fig. 1B). To complete the etching procedure the microcathode was drawn out from the solution with a uniform velocity in about 5 s. By varying the velocity, it was possible to change the shape and the tip dimensions, and with a little practice we easily obtained tips with a diameter of 1 µm or less.

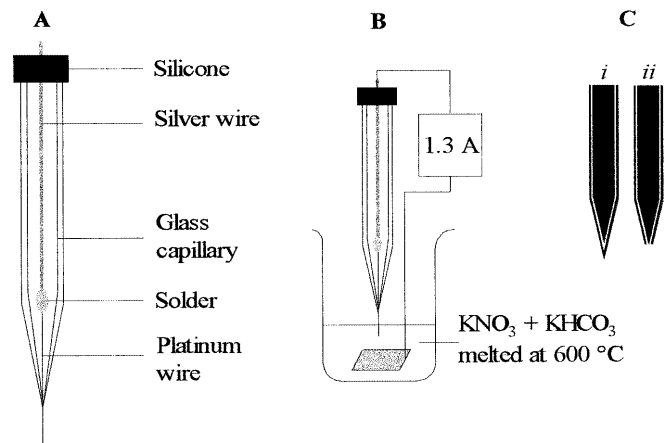


Fig. 1A–C. Schematic presentation of the stages involved in the fabrication of platinum microelectrodes. **A** A platinum wire electrode is produced. **B** The platinum wire is etched to a fine point. **C** The electrode is insulated by the electrodeposition of paint (*i*) and, after curing, is cut with a fresh surgical scalpel blade to expose a microscopic active area (*ii*). For details, see *Materials and methods*

Microwire insulation was achieved using an anodic electro-deposition paint (Glassphor ZQ 84-3225; BASF). The cell consisted of a platinum spiral (cathode) surrounding the Pt microwire, which served as the anode. A constant voltage was applied (+3 V for 30 s). After removing the tip from the solution (Fig. 1C *i*), hardening of the coating was achieved at 200 °C for 180 s. To expose a disk-shaped electroactive surface area, the insulated platinum wire was fixed with modelling clay onto a microscope slide. It was important to place the platinum wire nearly in parallel and in contact with the glass surface. Cutting was carried out with a fresh surgical scalpel blade. The cut end was examined at high magnification, and only if it looked smooth was it used for the measurements.

The oxygen probe was completed with a platinum wire 10 mm long and 0.5 mm in diameter acting as the auxiliary electrode and with a reference half-cell Ag/AgCl/0.1 M KNO₃ + NaCl 0.08 M. The cell was arranged in a three-electrode polarographic configuration which maintained the working microelectrode at a polarising voltage of -750 mV, ensuring a condition of diffusion limiting current for dissolved oxygen reduction.

Vibrating-microelectrode system. The design and mode of operation of the vibrating-microelectrode system were similar to those originally used by Shabala et al. (1997) and are described schematically in Fig. 2.

The O₂ microelectrodes were mounted on a manual micromanipulator providing three-dimensional positioning. During measurements the distance between the root surface and the electrodes was changed by fixing the measuring chamber on a three-way hydraulic micromanipulator (WR-6; Narishige, Tokyo, Japan) driven by computer-controlled stepper motors (type I 5PM-K004-01; Minebea Co., Tokyo, Japan). The electrodes were connected by screened cables to a potentiostat (custom-built based on an AD 645 JN operational amplifier; Analog Device, Norwood, Mass., USA) which supplied the polarising voltage. The output current was converted to voltage, amplified, low-pass-filtered, and connected via a multichannel A-D converter card (Lab-PC-1200; National Instruments, Austin, Tex., USA) to a P133 personal computer.

Measurements of the difference in electrode voltage at the two extremes of vibration was achieved by digitising the electrode signals and computing the potential difference. Data were collected at a rate of 1000 data points per second.

For each electrode position, the first 2 s after the movement began were automatically discarded to eliminate movement artefacts and to allow the electrochemical settling of the electrodes, the

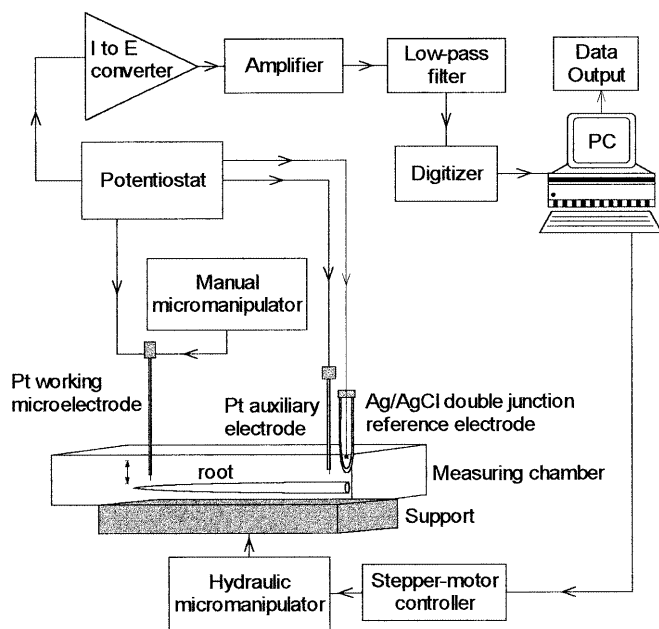


Fig. 2. Schematic diagram of the system and mode of operation for the 'vibrating microelectrode technique' (for details, see *Materials and methods*)

remaining signal was then averaged. The computer calculated the difference between this average and the previous one at the other extreme position and finally calculated a moving average of these differences over any desired time period.

Measurement of O_2 fluxes. Oxygen fluxes were calculated using Fick's first law of diffusion:

$$J = \frac{D(C_1 - C_2)}{\Delta x}$$

where J is the flux rate ($\text{mol cm}^{-2} \text{s}^{-1}$), D is the diffusion coefficient for O_2 ($2.51 \times 10^{-5} \text{ cm}^2 \text{ s}^{-1}$ at 25°C and 101.3 kPa), C_1 and C_2 are the concentrations at the two measurement positions and Δx is the distance of measurement (cm).

For the transport studies, *Olea europaea* leaves and roots were carefully washed with deionised water. A single root from the root system or a leaf attached to the plant was anchored to the bottom of the measuring chamber containing a $50 \mu\text{M}$ $\text{Ca}(\text{NO}_3)_2$ solution. Samples were secured to the chamber bottom using Plexiglas blocks fixed with silicone grease. A settling time of 1 h prior to the start of the experiment was allowed.

Experiments were performed at $25 \pm 1^\circ \text{C}$. Microelectrodes were set perpendicularly to the sample and a differential signal was calculated from data obtained while oscillating the electrode at 0.1 Hz between two points, $10 \mu\text{m}$ apart, such that the extremes of the vibration were usually between 1 and $11 \mu\text{m}$ from the tissue surface.

Results

Electrochemical behaviour of the microelectrodes. The platinum microelectrodes fabricated were initially tested in pure water or in $50 \mu\text{M}$ $\text{Ca}(\text{NO}_3)_2$ solution. Figure 3 shows the polarogram (graphs of current versus voltage) obtained with the expected sigmoidal response. When polarised with a voltage sweep from -0.9 to 0.2 V , oxygen microelectrodes showed a current plateau in the

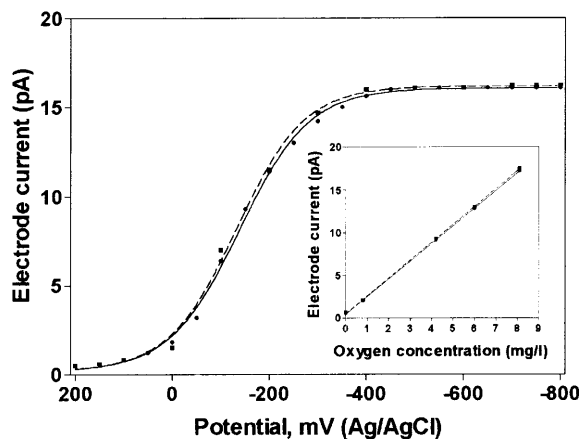


Fig. 3. A representative polarogram for the reduction of dissolved oxygen, showing the response of the microelectrode current to the applied potentials. The polarogram was obtained by placing the electrode in H_2O (—) or in a solution containing $50 \mu\text{M}$ $\text{Ca}(\text{NO}_3)_2$ (---). The inset shows a representative calibration plot of a microelectrode in H_2O (----) or in a solution containing $50 \mu\text{M}$ $\text{Ca}(\text{NO}_3)_2$ (—)

range -0.4 to -0.8 V with an output of approximately 20 pA (depending on the tip radius) in air-saturated pure water and of 0.5 – 1 pA in N_2 -saturated pure water. The presence of $50 \mu\text{M}$ $\text{Ca}(\text{NO}_3)_2$ in the solution had no effect on the behaviour of the microelectrode. During experiments, the microelectrode was polarised at a voltage of -750 mV , ensuring a condition of diffusion-limiting current for dissolved oxygen reduction, linearly dependent on O_2 concentration.

A calibration curve was then obtained by measuring the microelectrode current in water equilibrated with 100% N_2 or using pressurised gases containing 0, 1, 2, 3...21% O_2 , 1 ml l^{-1} CO_2 , and the balance N_2 (Fig. 3, inset). Also in this case the presence of $50 \mu\text{M}$ $\text{Ca}(\text{NO}_3)_2$ in the solution had no effect on the calibration curve.

The mass-transport-controlled limiting current i_{lim} , measured from the plateau region of the sigmoidal steady-state polarogram, can be related to the effective electrochemical radius of exposed metal by the following equation (Pendley and Abruña 1990):

$$i_{lim} = 4nFDC^*r$$

where F is Faraday's constant, n is the number of electrons transferred per redox event, D is the diffusion coefficient of the reactant ($\text{cm}^2 \text{ s}^{-1}$), C^* is the bulk concentration of the reactant (mol cm^{-3}) and r is the radius of the section of the tip. A tacit assumption implied in the use of this equation is that the electrode has a disk geometry. The assumption of other exposed metal geometries (such as a hemisphere or a cone) would yield electrode radii that would be 20 to 30% smaller than those obtained. Thus, this does not affect the primary conclusion that extremely small electrodes can be prepared by an etching-coating method. Using the above equation, we were able to calculate electrochemical radii ranging between 0.1 and $1 \mu\text{m}$, with more than 70% of the microelectrodes showing radii under $0.5 \mu\text{m}$. Scanning electron microscope images (data not shown)

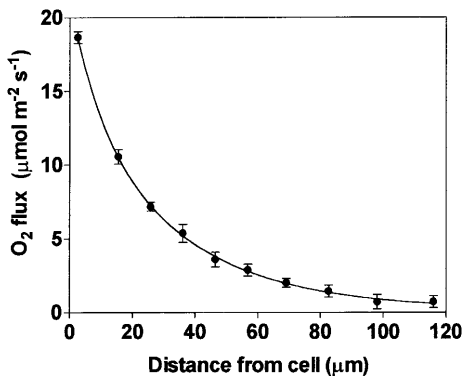


Fig. 4. Oxygen efflux in relation to the distance from a stomatal complex of *Olea europaea* measured along a line perpendicular to the plane. Each datum point is the mean \pm SE of 60 measurements

of the larger radii electrodes (1 μm) showed exposed metal apertures of dimensions that were in good agreement with the electrochemically determined electrode radii.

Oxygen fluxes in leaves. The ability of the system to detect oxygen fluxes is shown clearly by measuring the profile of the oxygen gradient above an individual stomatal complex (Fig. 4). Taking flux measurements at known distances from the stomata, along a line perpendicular to the plane, an exponential fall in oxygen fluxes was detected by moving the microelectrode outward until a stable level was reached at a distance of about 120 μm from the cells. The gradient, measured in an air-saturated solution, above the same stomatal complex, shows that the distance of vibration usually adopted for the microelectrodes (10 μm) lies entirely within the gradient.

When switching the light on and off it was possible to measure real-time changes in light-induced oxygen fluxes (Fig. 5). In the presence of light the photosynthetically generated O_2 diffusing through the stomata averaged (in 47 replicates of samples) $15 \pm 3 \mu\text{mol m}^{-2} \text{s}^{-1}$.

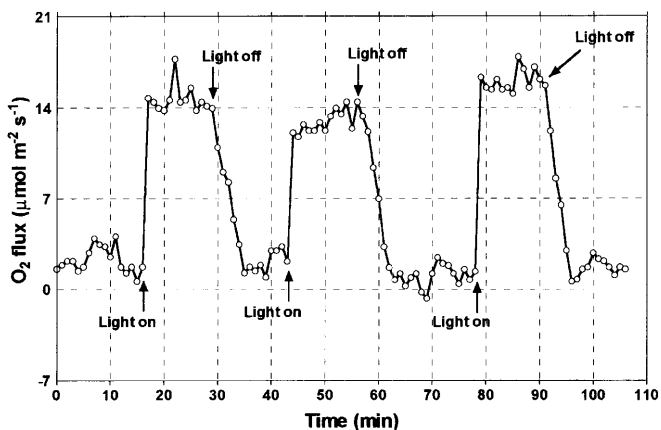


Fig. 5. A representative recording showing the real-time response of O_2 evolution from a single stomatal complex of *Olea europaea* in response to step changes in light ($700 \mu\text{mol photons m}^{-2} \text{s}^{-1}$) availability

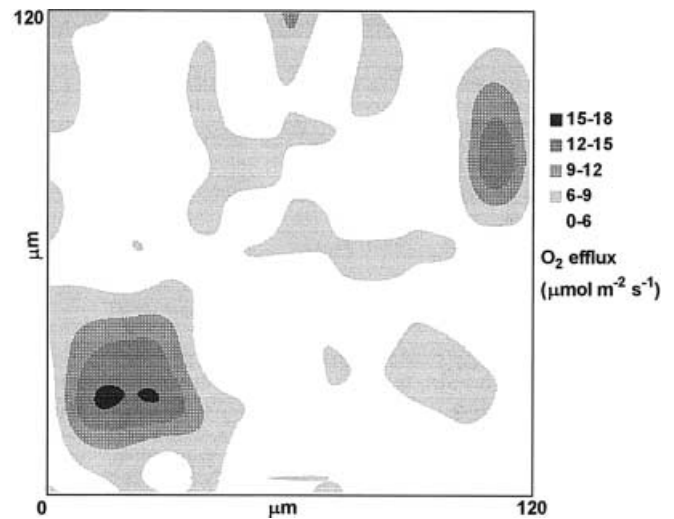


Fig. 6. Contour map showing the oxygen evolution from two different stomata of an illuminated leaf of *Olea europaea*. The data were recorded by oscillating the electrode as a square wave at 0.1 Hz between two points, 10 μm apart. The electrode was moved in the x direction collecting data every 2 μm . After finishing one pass, the microelectrode was moved 5 μm in the y direction and then returned in the opposite x direction

In addition to punctual flux measurements, the system can be used to monitor oxygen evolution from an illuminated leaf for a specific region. To obtain “topographical” images of the O_2 evolution, regions of the leaf ($120 \times 120 \mu\text{m}$) were scanned with the microelectrode. Figure 6 show an example of the results obtained. The two peaks correspond to the photosynthetically generated oxygen diffusing through two different stomata. The efflux values associated with these peaks are at least 3 times greater than the averaged background value.

Oxygen fluxes in roots. The sensitivity of the vibrating O_2 -selective microelectrode was further examined by measuring O_2 fluxes at different positions along an intact roots. In spite of some differences in the quantitative characteristics, all plants showed the same spatial organisation in net O_2 influxes. A representative trace of an O_2 flux profile along an *Olea europaea* root is shown in Fig. 7. Oxygen influxes showed two distinct peaks at 0.5–1 and 2–2.5 mm from the root apex. The first peak, in the division zone, averaged ($n = 38$) $38 \pm 5 \text{ nmol m}^{-2} \text{s}^{-1}$, while the second peak, in the elongation region averaged ($n = 38$) $68 \pm 6 \text{ nmol m}^{-2} \text{s}^{-1}$. At the more distal positions ($>3.5 \text{ mm}$) the O_2 influx was smaller ($21 \pm 2 \text{ nmol m}^{-2} \text{s}^{-1}$, $n = 39$) and remained constant even at positions as far back as 10 mm from the root apex.

In addition to the spatial organisation, the study of the oxygen fluxes also revealed the occurrence of clear dynamic phenomena. The observation of long-term records of O_2 fluxes measured in the region corresponding to the maximum influx zone (about 2.5 mm from the root apex) showed an oscillatory regime characterised by a fast oscillation with periods of about 8–9 min (Fig. 8)

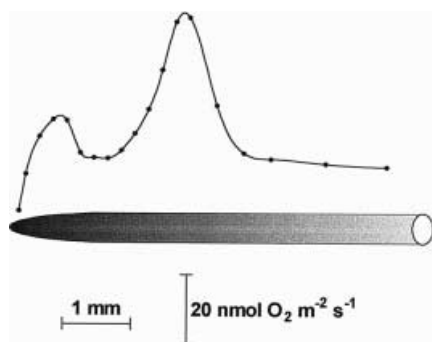


Fig. 7. Diagram illustrating the O_2 influx profile along a single root of *Olea europaea*. The data were recorded by oscillating the electrode perpendicularly to the root with an amplitude of $10\ \mu\text{m}$, such that the extremes of the vibration were between 1 and $11\ \mu\text{m}$ from the root surface. The position and magnitude of the fluxes are indicated by the data points. Each point represents the mean value of the O_2 flux over a time period of 10 min

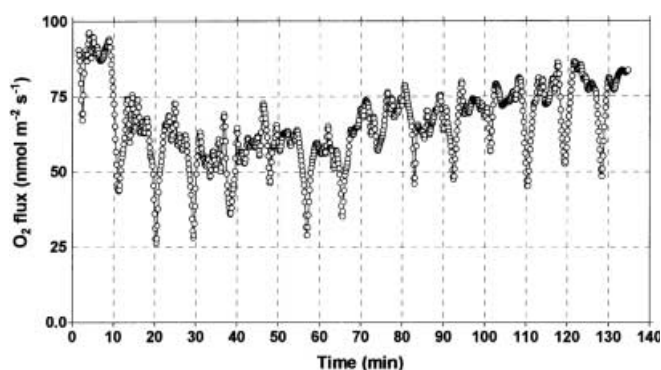


Fig. 8. Oscillatory behaviour of O_2 flux around the elongation region, $2.5\ \text{mm}$ from the root apex of *Olea europaea*. The oscillatory component is clearly shown

and an amplitude varying from a maximum of about 50 to about $0\ \text{nmol m}^{-2}\ \text{s}^{-1}$.

Discussion

In the present work we provide results that demonstrate the usefulness of a polarographic, oxygen-selective, vibrating-microelectrode system to map and measure extracellular oxygen gradients over distances as small as a few microns (depending on the radius of microelectrode) and for times as brief as a few seconds (depending on the frequency of vibration).

The only limiting factor of the spatial resolution of the system is represented by the dimension of the microelectrode tip, which, in the present work, has always been greater than $400\ \text{nm}$. In fact, microelectrodes with diameters under $400\ \text{nm}$ in some cases showed problems due both to mechanical instability and low signal-to-noise ratio.

With regard to the temporal resolution of the system, the limiting factor is the vibration frequency of the electrode, in turn linked to the response time of the microelectrode and to the time necessary to allow

diffusion to re-establish the gradient between movements. Since a polarographic platinum microcathode with these dimensions shows a virtually instantaneous response to the changes in concentration (the response time is under a microsecond; see for example Wightman 1988), one is limited only by the time needed for diffusion to re-establish a gradient after the electrode movements. In practice, vibration frequencies higher than $0.3\ \text{Hz}$ will result in an inaccurate measurement of the oxygen flux. Consequently, this technique will not record fast transient events, focusing instead on activities that last for several seconds.

An essential requirement for an electrode to be used in plant physiology, apart from a small overall physical dimension, is that the fabrication procedure is simple and convenient to perform with a relatively high success rate. The method of microelectrode fabrication detailed here offers three significant advantages. First, it is extremely quick and easy to fabricate microelectrodes. Second, the method allows for the construction of very small microelectrodes (typically with an outer diameter between 1 and $1.5\ \mu\text{m}$). Third, the success rate of constructing electrodes whose total outer diameter is less than $3\ \mu\text{m}$ has been about 90%. It should also be mentioned that platinum electrodes of extraordinarily small diameter can be prepared. For example, from the magnitude of the limiting current we estimated that about 10% of the electrodes fabricated had a diameter of about $300\ \text{nm}$.

According to Land et al. (1999), the most critical factor in the measurement of oxygen fluxes is the amplitude of the vibration, which must be contained entirely within the oxygen gradient. Extending the vibration amplitude beyond the range of the oxygen gradient would, in fact, result in an underestimation of the flux.

The measurements of oxygen evolution from a single stomatal complex were in good agreement with those obtained by the static electrode technique in *Olea europaea* (Bongi and Loreto 1989) and comparable to the oxygen rate expected for a woody plant (Zelitch 1971). Scanning an illuminated leaf region of about $120\ \mu\text{m} \times 120\ \mu\text{m}$ with an oxygen-selective microelectrode, we obtained “topographical” images of O_2 evolution from single stomata. Using Scanning electrochemical microscopy (SECM) Tsionsky et al. (1997) succeeded in obtaining results that, although qualitatively similar to ours, were quantitatively different because of the different experimental conditions. To maximise the resolution of SECM for detecting O_2 generated during photosynthesis, Tsionsky and co-workers (1997) utilised a reduced atmospheric O_2 (approximately 2%) instead of the normal (21%) O_2 concentration that we used in the present study.

The difference in the magnitude of the oxygen fluxes measured in different regions of the root suggests that distinct respiratory rates coupled to different energy requirements exist in the roots between the division and elongation zone. In the past year, ion flux profiles in roots of different plants have been reported. The spatial organisation of the uptake of Ca^{2+} (Ryan et al. 1990),

Cd^{2+} (Piñeros et al. 1998) and Mg^{2+} (Grunes et al. 1993) is characterised by a maximum influx zone in the elongation region (first millimetres behind the root apex). Accordingly, at least a fraction of the oxygen influx in this zone could be required for the generation of energy necessary for mineral nutrient acquisition by plants.

In addition to the spatial organisation, O_2 influx in roots revealed a pronounced rhythmical character. Shabala et al. (1997) showed oscillations in H^+ and Ca^{2+} fluxes around the elongation region of corn roots with periods of 7.84 and 7.77 min, respectively, in good agreement with our results showing O_2 oscillations with a period of 8.02 min. The same authors proposed that the rhythmic changes in H^+ fluxes relate to oscillations in the activities of electrogenic H^+ -ATPases. Accordingly, the oxygen oscillations could be linked to the same mechanism. However, these conclusions need to be confirmed in future experiments which are beyond the aim of the present work.

Gradmann and Hoffstadt (1998) demonstrated that, in a simplified model of a plant cell, fast oscillations of the transmembrane voltage are mostly due to the gating properties of Cl^- channels, whereas the fast oscillations are controlled by the effect of Cl^- concentration on the current. Unfortunately, the numerical parameters used, not tuned to produce realistic values, and the simple nature of the model do not allow comparisons with the oscillation parameters showed in the present study.

The detailed mechanisms at the origin of these rhythmical patterns, as for many oscillating phenomena in cellular biology, are at the moment not completely understood. One may speculate about the possible synchronising function for cell activity or in terms of intrinsic oscillatory models. In any case, the indisputable occurrence of fast oscillations with periods of some minutes in different phenomena ranging from plant growth (Kristie and Joliffe 1986) to ion fluxes, should be considered in future studies as overcoming the classical steady states of many laboratory experiments.

The spatial organisation and periodicity of oxygen influx in roots are topics worthy of more detailed investigation. If the phenomena are found to occur generally under experimental and natural conditions, there will be important questions about the validity of determinations integrating fluxes over the entire surface of the roots, especially in studies involving the plant response under certain conditions in which O_2 availability may limit respiration and growth, such as during flooding stress.

In conclusion, the experimental system was capable of measuring oxygen fluxes in specific locations of leaves and roots. The combination of topographic and electrochemical information on a micrometer scale makes the system an efficient tool with which to study biological phenomena involving oxygen diffusion. Consequently, there are a number of fruitful areas of research to be pursued with the oxygen-selective system presented. The mechanism behind stomatal movements, i.e. the regulation of guard-cell turgor by calcium, the response of stomata to CO_2 , and the heterogeneity of the stomatal aperture over the leaf surface, are among the most obvious possibilities.

References

- Armstrong W (1994) Polarographic oxygen electrodes and their use in plant aeration studies. *Proc R Soc Edinburgh* 102B: 511–527
- Bard AJ, Fan FRF, Kwak J, Lev O (1989) Scanning electrochemical microscopy: introduction and principles. *Anal Chem* 61: 132–138
- Bongi G, Loreto F (1989) Gas-exchange properties of salt-stressed olive (*Olea europaea* L.) leaves. *Plant Physiol* 90: 1408–1416
- Frateur I, Bayet E, Keddam M, Tribollet B (1999) Local redox potential measurement. *Electrochem Commun* 1: 336–340
- Gradmann D, Hoffstadt J (1998) Electrocoupling of ion transporters in plants: interaction with internal ion concentrations. *J Membr Biol* 166: 51–59
- Grunes DL, Ohno T, Huang JW, Kochian LV (1993) Effects of aluminium on magnesium, calcium, and potassium in wheat forages. In: Golf S, Dralle D, Vecchiet L (eds) *Magnesium 1993*. John Libbey & Co., London, pp 79–88
- Jaffe LF, Nuccitelli R (1974) An ultrasensitive vibrating probe for measuring steady extracellular currents. *J Cell Biol* 63: 614–628
- Kochian LV, Shaff JE, Kührtreiber WM, Jaffe LF, Lucas WJ (1992) Use of an extracellular ion-selective vibrating microelectrode system for the quantification of K^+ , H^+ , Ca^{2+} fluxes in maize roots and maize suspension cells. *Planta* 188: 601–610
- Kristie DN, Joliffe PA (1986) High-resolution studies of growth oscillations during stem elongation. *Can J Bot* 64: 2399–2405
- Land SC, Porterfield DM, Sanger RH, Smith PJS (1999) The self-referencing oxygen-selective microelectrode: detection of transmembrane oxygen flux from single cells. *J Exp Biol* 202: 211–218
- Ober ES, Sharp RE (1996) A microsensor for direct measurements of O_2 partial pressure within plant tissue. *J Exp Bot* 296: 447–454
- Pendley BD, Abruña HD (1990) Construction of submicrometer voltammetric electrodes. *Anal Chem* 62: 782–784
- Penner RM, Heben MJ, Longin TL, Lewis NS (1990) Fabrication and use of nanometer-sized electrodes in electrochemistry. *Science* 250: 1118–1121
- Piñeros MA, Shaff JE, Kochian LV (1998) Development, characterization, and application of a cadmium-selective microelectrode for the measurement of cadmium fluxes in roots of *Thlaspi* species and wheat. *Plant Physiol* 116: 1393–1401
- Ryan PR, Shaff JE, Kochian LV (1990) Ion fluxes in corn roots measured by microelectrodes with ion-specific liquid membranes. *J Membr Sci* 53: 59–69
- Shabala SN, Newman IA (1998) Osmotic sensitivity of Ca^{2+} and H^+ transporters in corn root: effects on fluxes and their oscillations in the elongation region. *J Membr Biol* 161: 45–54
- Shabala SN, Newman IA (1999) Light-induced changes in hydrogen, calcium, potassium, and chloride ion fluxes and concentrations from the mesophyll and epidermal tissues of bean leaves. Understanding the ionic basis of light-induced bioelectrogenesis. *Plant Physiol* 119: 1115–1124
- Shabala SN, Newman IA, Morris J (1997) Oscillations in H^+ and Ca^{2+} ion fluxes around the elongation region of corn roots and effects of external pH. *Plant Physiol* 113: 111–118
- Shabala SN, Newman IA, Whittington J, Juswono U (1998) Protoplast ion fluxes: their measurements and variation with time, position and osmoticum. *Planta* 204: 146–152
- Tsionsky M, Cardon ZG, Bard AJ, Jackson RB (1997) Photosynthetic electron transport in single guard cells as measured by scanning electrochemical microscopy. *Plant Physiol* 113: 895–901
- Whalen WJ, Riley J, Nair P (1967) A microelectrode for measuring intracellular PO_2 . *J Appl Physiol* 23: 798–801
- Wightman RM (1988) Voltammetry with microscopic electrodes in new domains. *Science* 240: 415–420
- Zelitch I (1971) Photosynthesis, photorespiration and plant productivity. Academic Press, New York